

Electronic Supplementary Information (ESI)

An Amide-Based Gel Polymer Electrolyte for Li-O₂ Batteries: Advancing Towards Practical Li-Air Batteries

Qinming Zhang^a, Xu Hu^a, Zhaojun Xie^{*a} and Zhen Zhou^{a,b}

^a School of Materials Science and Engineering, Institute of New Energy Material Chemistry, Key Laboratory of Advanced Energy Materials Chemistry (Ministry of Education), Renewable Energy Conversion and Storage Center (ReCast), Nankai University, Tianjin 300350, China. E-mail: zjxie@nankai.edu.cn

^b Interdisciplinary Research Center for Sustainable Energy Science and Engineering (IRC4SE²), School of Chemical Engineering and Energy, Zhengzhou University, Zhengzhou 450001, China. E-mail: zhenzhou@zzu.edu.cn

Experimental Section

Preparation of GPEs

N-phenylmethacrylamide (PMA, TCI, >98.0%) and LK-001 electrolyte (1 M LiTFSI/TEGDME, DodoChem) were mixed with mass ratios of 1:1, 1:2, 1:3, 1:4 and 1:5, and appropriate amounts of lithium bis(trifluoromethanesulfonyl)imide (LiTFSI, TCI, >98.0%) were added to maintain the volume concentration of the electrolytes (1 M), and 0.2 wt% 2,2'-Azobis(2-methylpropionitrile) (AIBN, Aladdin, 99%) was used as an initiator. The mixtures were absorbed by a glass fiber (GF/D, Whatman) separator and kept warm overnight at 60 °C to obtain a clear gel. The above operations were all completed in a glove box filled with Ar, with the water and oxygen contents controlled below 0.1 ppm. The as-prepared electrolytes were denoted as P1, P2, P3, P4 and P5, respectively.

Characterizations

Scanning electron microscope (SEM) images were taken by JSM-7800 and the attached energy-dispersive X-ray spectrometry (EDS) was utilized to obtain the elemental distribution information. Fourier transform-infrared (FT-IR) spectroscopy measurements were performed using a Brook ALPHA FTIR spectrometer. X-ray photoelectron spectroscopy (XPS) measurements were taken by Thermo Scientific ESCALAB 250Xi. XRD patterns were obtained using a Rigaku D/Max-2500 X-ray diffractometer with Cu K α radiation ($\lambda = 1.5406 \text{ \AA}$) at a scanning rate of $10^\circ \text{ min}^{-1}$. XPS analysis was operated on Thermo Scientific ESCALAB 250Xi.

Electrochemical Measurements

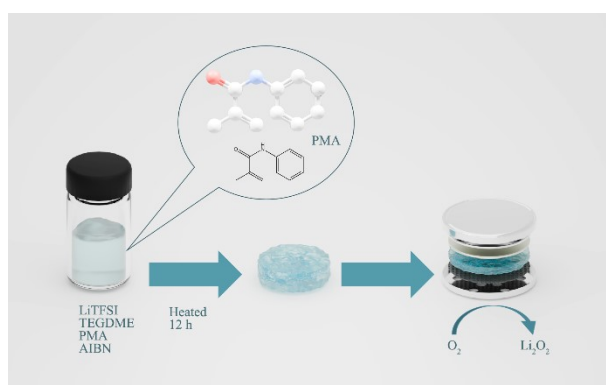
CR2032 coin-type cells were assembled in the above-mentioned glove box with or without holes on cathode shells according to whether oxygen was required in different tests. The cathode was prepared by coating a slurry composed of polyvinylidene fluoride (PVDF) and Ketjen black (KB) with a mass ratio of 1:9 onto a carbon paper (12 mm in diameter), and the active material mass loading was 0.25 mg cm^{-2} .

A typical cell consisted of a lithium anode, a glassfiber separator with LEs or GPEs and a KB cathode. All cells were stabilized for 5 h before electrochemical measurements on LAND-CT2001A testers or LSV and CV measurements on a CHI760E electrochemical workstation.

All measurements were performed at room temperature.

Computational details related to DS-PAW

The binding energies of O_2 on the monomer of PMA and TEGDME were calculated using DS-PAW¹ software. Perdew-Burke-Ernzerhof (PBE) functional² within the generalized gradient approximation was used to describe the exchange-correlation interaction. A single gamma-centered Monkhorst-Pack scheme³ was applied for structure relaxation due to the large cell ($40 \times 40 \times 40 \text{ \AA}^3$) used. 520 eV was used as the energy cutoff for the plane-wave basis set. Van der Waals (vdW) interactions were included using Grimme's DFT-D3 method with zero damping⁴. The convergence criteria for the electronic self-consistent field calculations and the ionic relaxation loop were set to 10^{-5} eV and 0.05 eV/\AA , respectively.



Scheme 1 A schematic diagram regarding the synthesis of a PPMA GPE and the assembly of the Li-O₂/air battery.

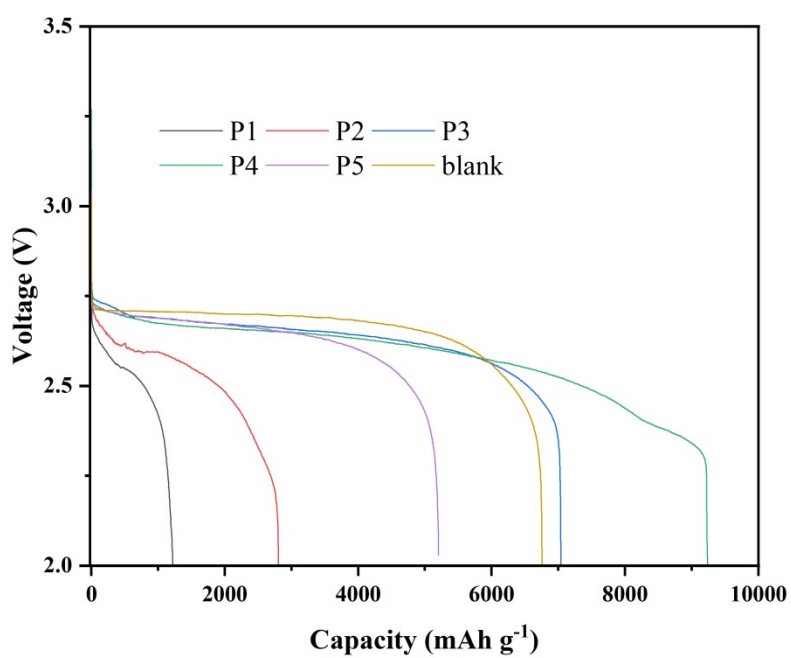


Fig. S1. Discharge curves of Li-O₂ batteries with different electrolytes at 200 mA g⁻¹.

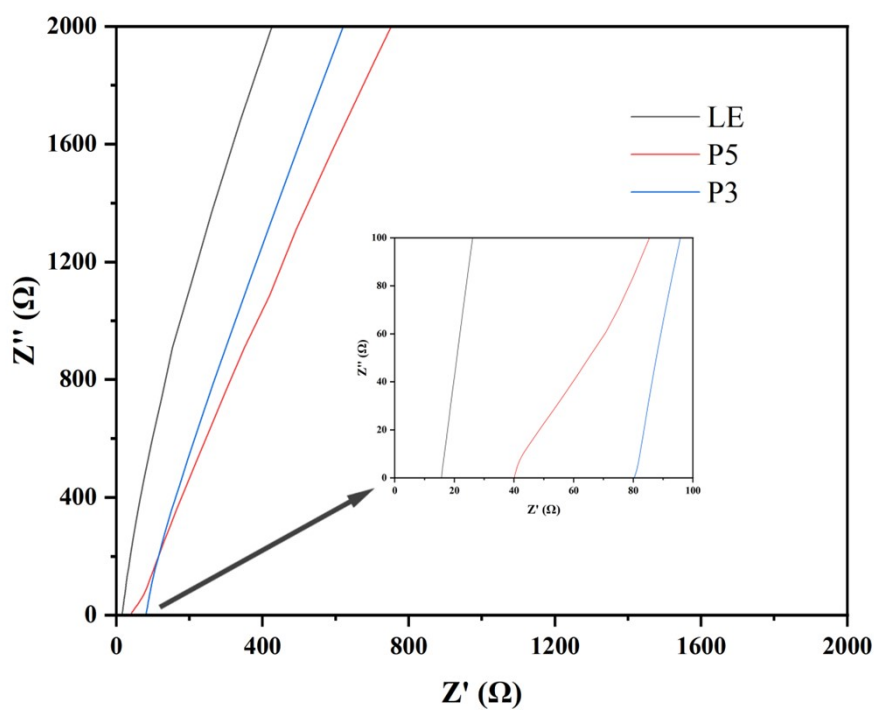


Fig. S2. Nyquist plots for EIS measurements of different electrolytes.

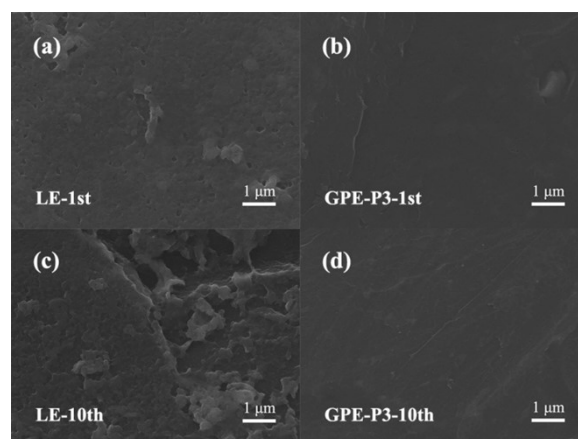


Fig. S3. SEM images of Li anodes after stripping and deposition in symmetric cells.

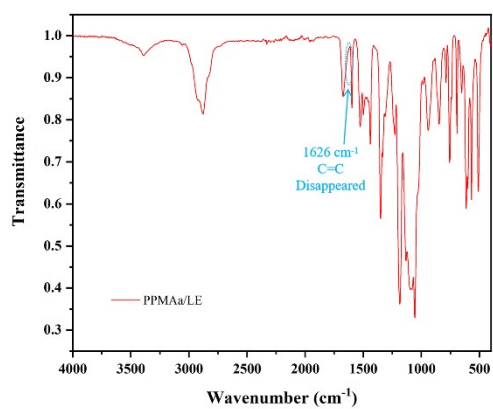
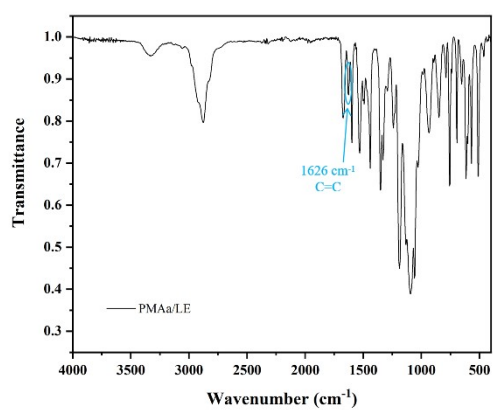


Fig. S4 FT-IR spectroscopy of GPE-P3 (a) before and (b) after polymerization.

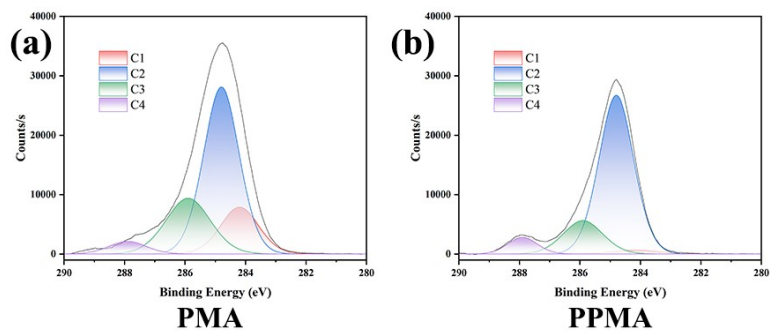


Fig. S5. XPS of PMA and PPMA (a) before and (b) after polymerization.

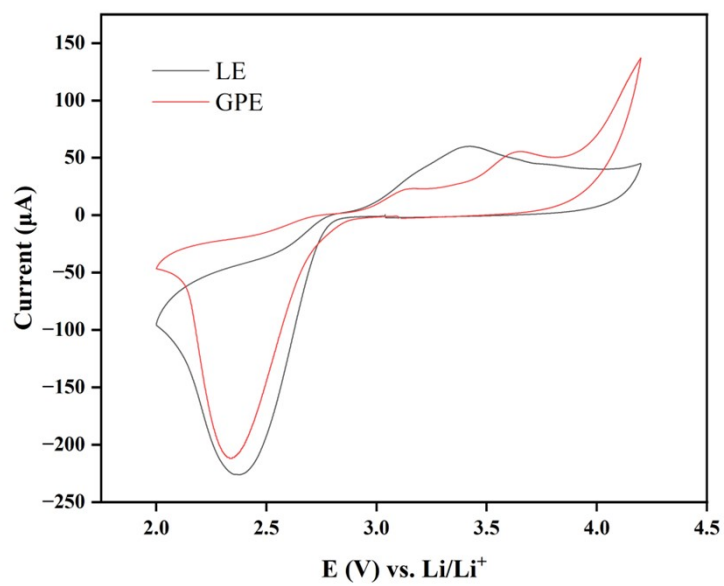


Fig. S6. CV curves of Li-O₂ batteries with LEs or GPE-P3.

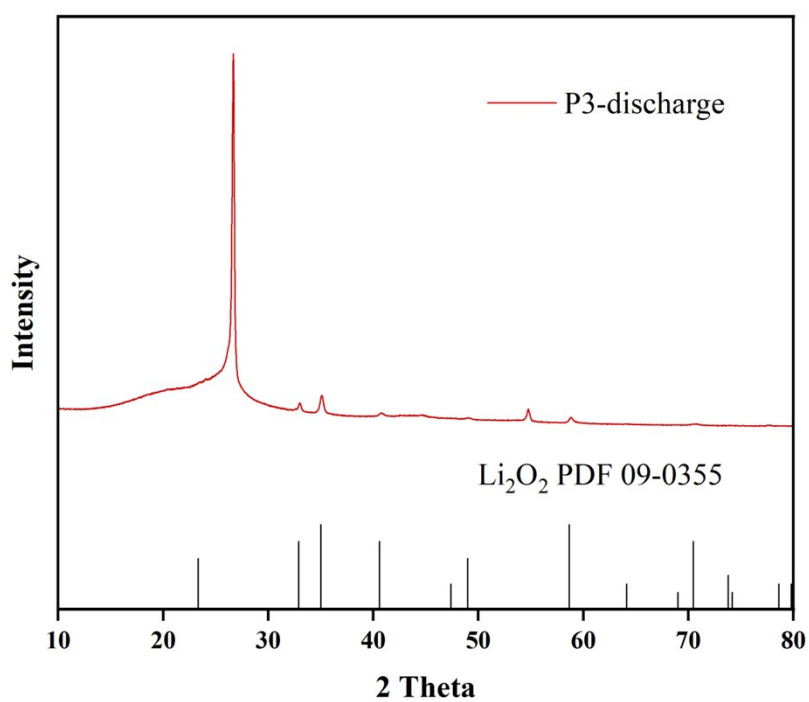


Fig. S7. XRD patterns of Li-O₂ batteries with GPE-P3 and standard PDF card of Li₂O₂.

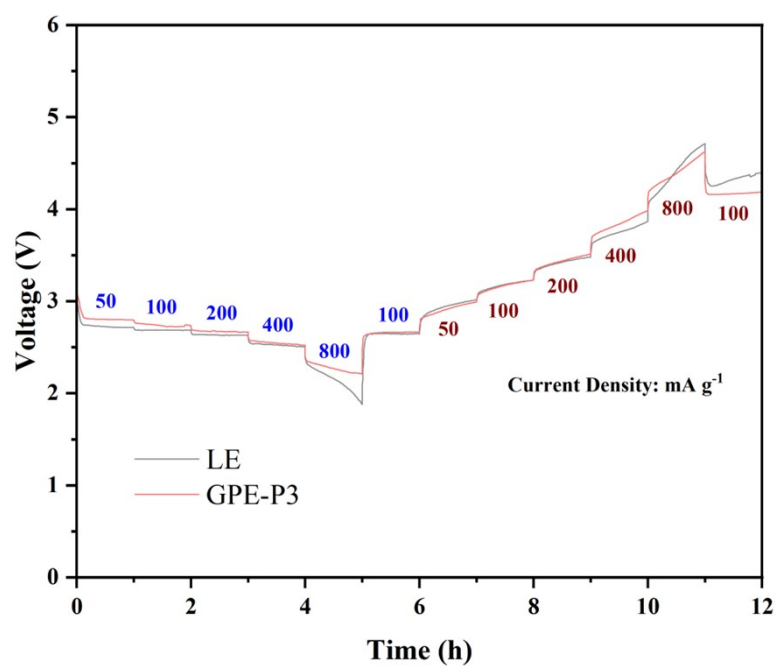


Fig. S8. Rate performance for Li-O₂ batteries with GPE-P3 or liquid electrolyte (LE).

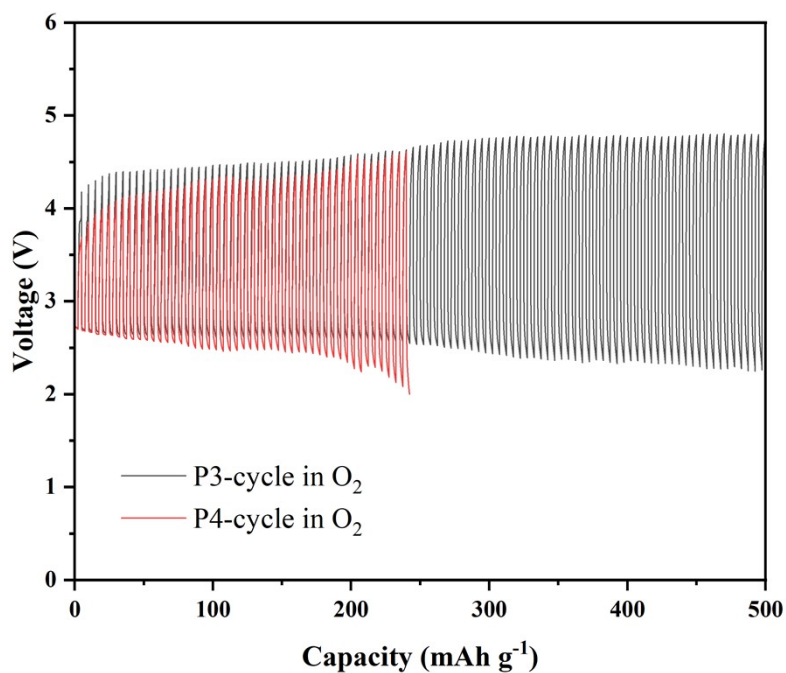


Fig. S9. Cycling curves of Li-O₂ batteries with GPE-P3 or P4 under 200 mA g⁻¹.

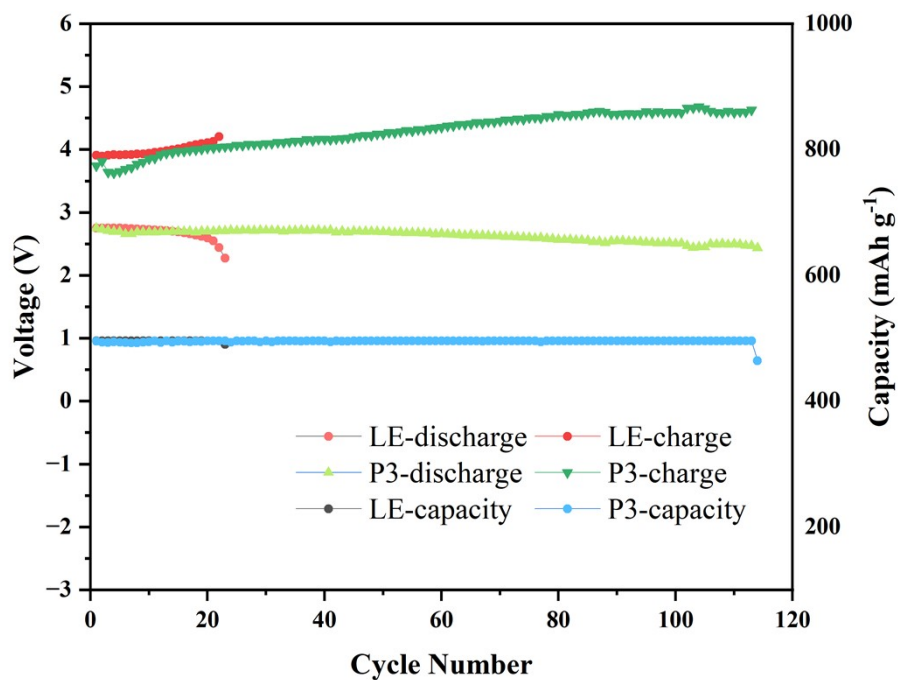


Fig. S10. Cycling performance of Li-O₂ batteries with LE or GPE-P3 under current

density of 100 mA g^{-1} with cut-off capacity of 500 mAh g^{-1} .

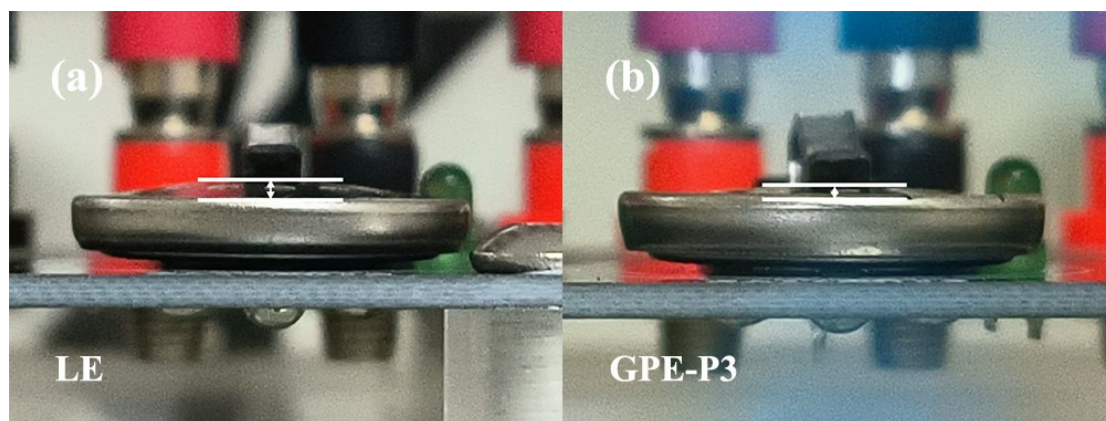


Fig. S11. Comparison of volume expansion of Li-O₂ batteries with LEs or GPE-P3 after 20 cycles of discharge and recharge.

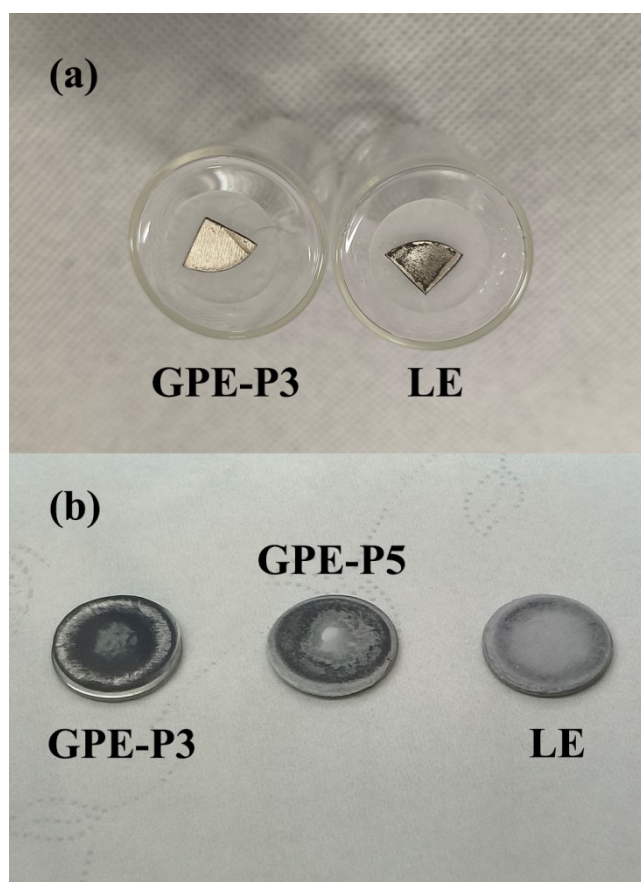


Fig. S12. Photos of Li anodes: (a) covered with different electrolytes and exposed to air for several hours, and (b) after cycling in O₂.

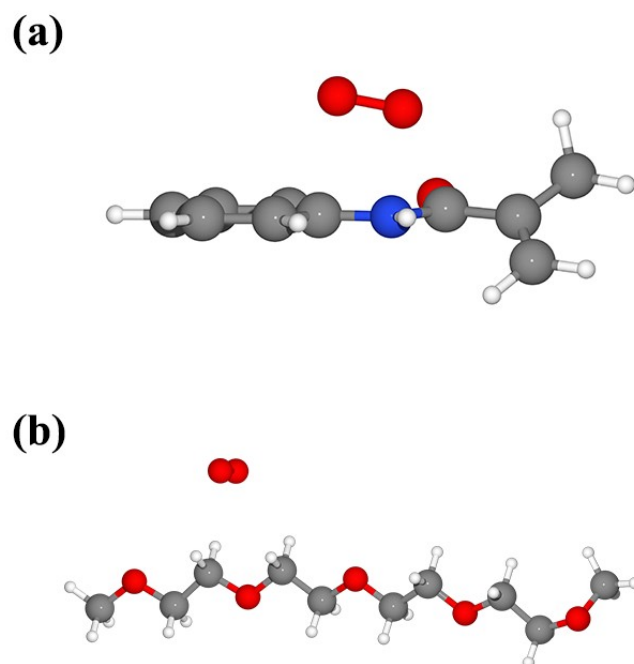


Fig. S13. Optimized atomic structures of O_2 on the monomer of (a) PMA and (b) TEGDME.

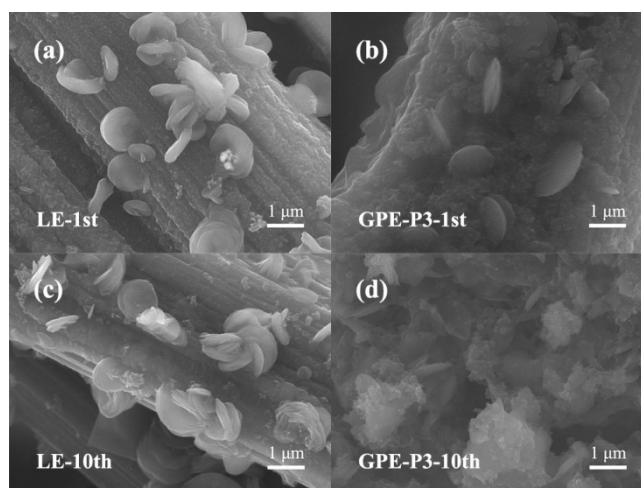


Fig. S14. SEM images of discharge products in $Li-O_2$ batteries after 1 cycle and 10 cycles.

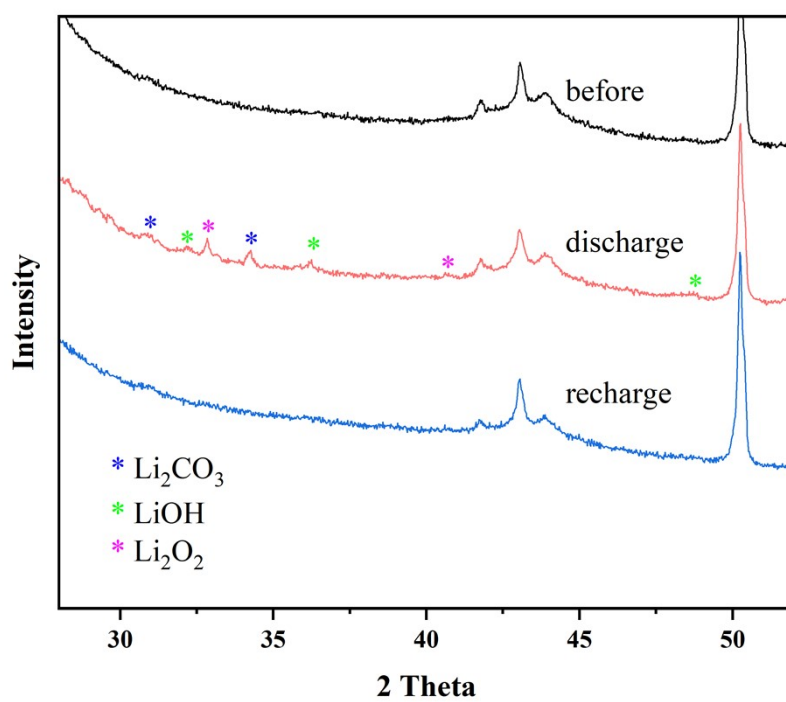


Fig. S15. XRD patterns of Li-air battery cathodes with GPE-P3 before discharge, after discharge and after recharge.

Table S1. Ionic conductivities of different electrolytes calculated based on EIS data.

	Bulk Resistance (Ω)	Ionic Conductivity (S cm ⁻¹)
LE	15.72	4.13×10^{-3}
GPE-P5	40.10	1.62×10^{-3}
GPE-P3	80.29	8.10×10^{-4}

Table S2. Assignment of various peaks for XPS in Fig. R2.

Peak	Assignment	Binding Energy (eV)
C1	C=C	284.2
C2	C-C	284.8
C3	C-N	285.9
C4	C=O	287.9

Table S3. DFT-calculated energies of O₂ on monomers of PMA and TEGDME.

	Total energy / eV
monomer of PMA	-2451.351
TEGDME	-4111.154
O ₂ on monomer of PMA	-3325.072
O ₂ on TEGDME	-4984.660
O ₂	-873.459

Table S4. Performance comparison with previous reports.

	Atmosphere	Current Density & Cut-off Capacity	Cycles	Operating Time (h)
This Work	O ₂	200 mA g ⁻¹ 500 mAh g ⁻¹	127	635
5	O ₂	312.5 mA g ⁻¹ 1250 mAh g ⁻¹	194	1552
6	O ₂	0.1 mA cm ⁻² 1 mAh cm ⁻²	34	680
7	O ₂	200 mA g ⁻¹ 500 mAh g ⁻¹	70	350
8	O ₂	0.05 mA cm ⁻² 0.25 mAh cm ⁻²	117	1170
9	O ₂	0.1 mA cm ⁻² 0.4 mAh cm ⁻²	39	312
10	O ₂	500 mA g ⁻¹ 1000 mAh g ⁻¹	250	1000
11	O ₂	250 mA g ⁻¹ 500 mAh g ⁻¹	55	220
This Work	Air	200 mA g ⁻¹ 500 mAh g ⁻¹	120	600
12	Air	500 mA g ⁻¹ 500 mAh g ⁻¹	100	200
13	Air	200 mA g ⁻¹ 500 mAh g ⁻¹	235	1175
14	Air	500 mA g ⁻¹ 1000 mAh g ⁻¹	241	964
15	Air	500 mA g ⁻¹ 1000 mAh g ⁻¹	98	196

References

1. P. E. Blöchl, *Phys. Rev. B*, 1994, **50**, 17953.
2. S. Grimme, J. Antony, S. Ehrlich and H. Krieg, *J. Chem. Phys.*, 2010, **132**, 154104.
3. H. J. Monkhorst and J. D. Pack, *Phys. Rev. B*, 1976, **13**, 5188.
4. J. P. Perdew, K. Burke and M. Ernzerhof, *Phys. Rev. Lett.*, 1996, **77**, 3865.
5. C. Zhao, Q. Sun, J. Luo, J. Liang, Y. Liu, L. Zhang, J. Wang, S. Deng, X. Lin and X. Yang, *Chem. Mater.*, 2020, **32**, 10113-10119.
6. M. Celik, S. Pakseresht, A. W. M. Al-Ogaili, S. Usta, H. Akbulut and T. Cetinkaya, *Batteries Supercaps*, 2023, **6**, e202300263.
7. K.-N. Gao, H.-R. Wang, M.-H. He, Y.-Q. Li, Z.-H. Cui, Y. Mao and T. Zhang, *J. Power Sources*, 2020, **463**, 228179.
8. H. Zhao, X. Liu, Z. Chi, S. Chen, S. Li, Z. Guo and L. Wang, *Appl. Surf. Sci.*, 2021, **565**, 150612.
9. Z. Gu, X. Xin, J. Yang, D. Guo, S. Yang, J. Wu, Y. Sun and X. Yao, *ACS Appl. Energy Mater.*, 2022, **5**, 9149-9157.
10. X. Zou, Q. Lu, Y. Zhong, K. Liao, W. Zhou and Z. Shao, *Small*, 2018, **14**, 1801798.
11. A. Chamaani, M. Safa, N. Chawla and B. El-Zahab, *ACS Appl. Mater. Interfaces*, 2017, **9**, 33819-33826.
12. J. Li, Z. Wang, L. Yang, Y. Liu, Y. Xing, S. Zhang and H. Xu, *ACS Appl. Mater. Interfaces*, 2021, **13**, 18627-18637.
13. X. Lei, X. Liu, W. Ma, Z. Cao, Y. Wang and Y. Ding, *Angew. Chem. Int. Ed.*, 2018, **57**, 16131-16135.
14. Z. W. Li, Y. L. Liang, J. Wang, J. M. Yan, J. W. Liu, G. Huang, T. Liu and X. B. Zhang, *Adv. Energy Mater.*, 2024, **14**, 2304463.
15. Y. B. Kim, I. T. Kim, M. J. Song and M. W. Shin, *J. Membrane Sci.*, 2018, **563**, 835-842.